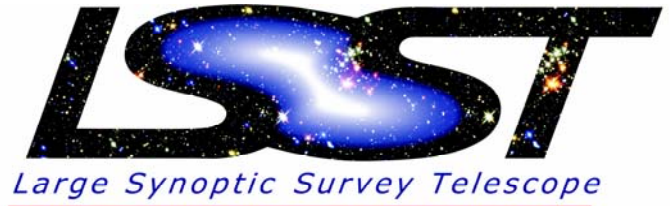


Observational Validation of LSST Image Quality Requirements



S. Asztalos (LLNL), D. Burke (SLAC), C. F. Claver (NOAO), S. Heathcote (SOAR, NOAO), L. Rosenberg (LLNL), A. Becker (U. Washington), M. Britton, B. Ellerbroek (Cal Tech), K. Gilmore (SLAC), M.-C. Hainaut-Rouelle (Gemini), G. Jernigan (Berkeley SSL and SLAC), S. M. Kahn (SLAC), V. Krabbendam (NOAO), V. Margoniner (UC Davis), D. Monet (USNO), J. R. Peterson (SLAC), P. Pinto (U. Arizona), P. Puxley, P. Puxley (Gemini), A. Rasmussen (SLAC), J. Sebag (NOAO), L. Simms (SLAC), A. Tokovinin (NOAO), J.A. Tyson, D. Wittman (UC Davis)

Cosmic shear provides a suite of completely independent methods of probing dark energy. The LSST statistical errors on the shear power spectrum will be very small, so keeping systematic errors below this level will be a challenge. Here we investigate one systematic: the atmosphere, which will inject spurious power on small scales. Foreground stars are used to fit and remove such seeing induced correlations. An investigation using the 8-m Subaru telescope with LSST-like exposure times shows that the shear residuals from the atmosphere are comfortably less than the expected statistical errors. Discretionary time on the Gemini telescope in conjunction with site MASS-DIMM data was obtained to further explore the effects of seeing on object ellipticity. We find that ellipticity correlations which extend out to 1' under good seeing conditions vanish when the seeing approaches 1". Scales larger than 1' are most important for cosmology, and at these scales the correlations are small in all seeing conditions. Finally, we present results on wind direction and ellipticity correlation length.

The issue: Galaxies have intrinsic shape characteristics, such as the orientation of their major and minor axes, that are randomly distributed. Intervening dark matter clumps induce source galaxy tangential shape alignments (shear) that are correlated over angles (tens of arcminutes) large compared with the mean separation of these galaxies. In the limit of weak gravitational lensing this signal is small (0.1%) compared with the intrinsic galaxy ellipticity. The problem is compounded by other effects that mimic shear signal, such as the atmosphere. In particular, turbulent cells of differing orientation and strength pass are projected onto different parts of aperture during an exposure, causing PSF anisotropy. Techniques which exist to remove this effect are limited by the spacing of bright stars at high galactic altitudes. An open question is whether the atmosphere is correlated over the typical separation of high-altitude stars ~ 0.5'

To explore this question we have adopted code (Arroyo) written for the Thirty Meter Telescope to simulate monochromatic radiation emitted from a grid of stars. Arroyo allows for the inclusion of an arbitrary number of atmospheric phase screens with varying strengths and altitudes. The user may choose between geometric or diffractive propagation. Fig.1 are successive snapshots of the point spread functions (PSFs) from a single star separated by 1 s intervals.

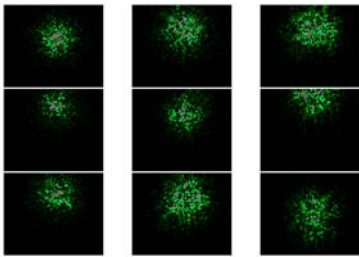


Fig.1 Nine successive snapshots of the PSF of a single star separated by 1.0 s. The initially planar wavefront is corrupted by a single atmospheric ground layer. Gross motion of the PSF centroid is due to sampling different regions of the phase screen.

To simulate the anticipated atmospheric correlation length a 15x15 grid of stars was constructed. Wavefronts were propagated through six turbulent phase screens via FFT to the focal plane. For each star a total of 10 snapshots separated by 1 s were co-added to approximate the LSST exposure time. The x- and y-ellipticities all 225 stars were measured in the co-added image and the vector ellipticity residual computed for all N(N-1)/2 distinct pair. The top plot of Fig 2 shows the ellipticity residual for the 252,00 pair as a function of separation computed in this fashion. The bottom plot shows the average residual.

Validation: The above results show that atmospheric correlations should persist beyond the nominal 1' required for PSF interpolation. To test the validity of these simulations data was acquired at the GMOS.

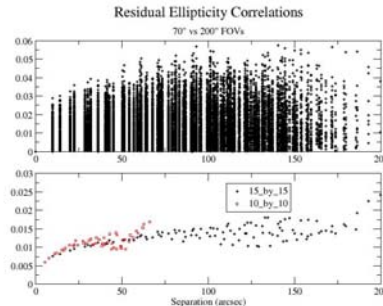


Fig. 2 (Top) Vector ellipticity residuals as a function of separation in arcsec for all distinct combinations of a 15x15 grid of stars, each separated by 5". Gaps appear because of the discrete star spacing. (Bottom) Same as the upper plot, but with the data placed into 2" bins, then averaged. The red squares are for a 10x10 grid of stars under identical conditions.

instrument at Gemini-South in May, 2005. 43 images were taken in the r-band over two fields separated by 84° in RA over the course of 4 evenings. Simultaneous atmospheric data were taken using local MASS/DIMM instruments.

The top plot in Fig 3 shows MASS and DIMM measured seeing at the time of each exposure, along with the seeing computed from each image using the IRAF gemseeing routine. In addition, on the right axis is the number of objects above threshold determined by SExtractor as a proxy for cloud cover. The MASS and DIMM instruments measure free-atmospheric and total seeing, respectively. The lower plot shows the turbulence intensity at each of the six atmospheric layers as determined by the MASS instrument. These data will be utilized in planned validation simulations of the atmosphere.

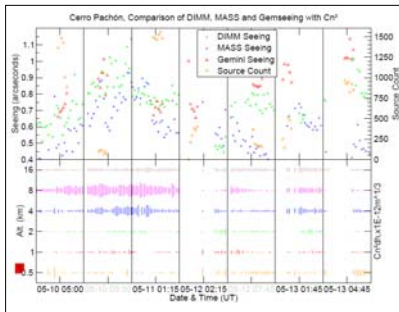


Fig. 3 (Top) MASS and DIMM estimates of the free- and total seeing for each of the 43 exposures. Estimates of the seeing extracted from the images (red) are in good agreement with the DIMM results. (Bottom) The turbulence intensities as a function of altitude as determined by the MASS instrument.

Analysis: Following the procedure leading to Fig. 2, ellipticity residuals were computed for 33 images having the same RA and DEC and the results binned according to the seeing as determined from gemseeing. This result is shown below in Fig 4.

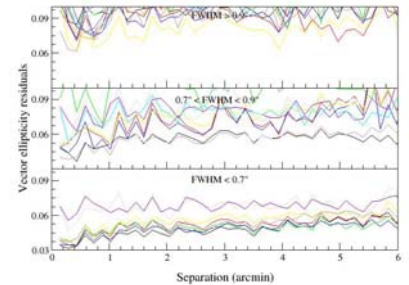


Fig. 4 Vector ellipticity residuals for 33 GMOS images binned by seeing extracted from the Gemini IRAF routine gemseeing. Each color represents the residuals from a different image. For good seeing correlations persist across the 5.6' field of view.

For good seeing (~0.7") correlations persist over the entire field a view. This was confirmed by reconstructing the lower plot in Fig. 5, but instead randomizing the position and ellipticity angle for all detected objects. We are investigating the degree, if any, to which shot noise contributes to the ellipticity for images taken under poorer seeing conditions.

Besides atmospheric turbulence intensities as a function of altitude, simulations require wind velocities as input. Unlike MASS and DIMM data, which are acquired on site, meteorological wind data is more difficult to access. We have investigated extraction of the wind direction directly from the images themselves and find good correlation between minima in the ellipticity residual with wind direction. Fig. 5 shows this result from the same GMOS images described above.

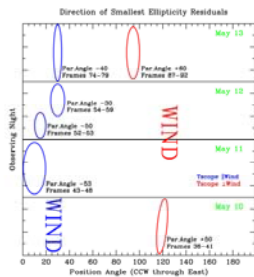


Fig. 5 Position angle for each frame for which the smallest residuals are projected along the y-axis. These minima correlate well with the projected ground-layer wind direction across the detector, as indicated in red and blue for the two different observational setups above.